In ovo chorioallantoic membrane assay as a xenograft model for pediatric rhabdomyosarcoma

CHIKA SHOJI[1], KEN KIKUCHI[1,2], HIDEKI YOSHIDA[1], MITSURU MIYACHI[1], SHIGEKI YAGYU[1], KUNIHIKO TSUCHIYA[1], TAKAAKI NAKAYA[3], HAJIME HOSOI[1,4] and TOMOKO IEHARA[1]

[1]Department of Pediatrics, Graduate School of Medical Science, Kyoto Prefectural University of Medicine, Kyoto 602-8566; [2]Department of Pediatrics, Uji Takeda Hospital, Uji, Kyoto 611-0021; [3]Department of Infectious Diseases, Graduate School of Medical Science, Kyoto Prefectural University of Medicine, Kyoto 602-8566; [4]Department of Nursing, Doshisha Women's College of Liberal Arts, Kyotanabe, Kyoto 610-0395, Japan

Received July 22, 2022; Accepted December 15, 2022

DOI: 10.3892/or.2023.8513

Abstract. Rhabdomyosarcoma (RMS) is the most common highly malignant pediatric soft tissue sarcoma. While recent multidisciplinary treatments have improved the 5-year survival rate of low/intermediate-risk patients to 70-90%, there are various complications that arise due to treatment-related toxicities. Immunodeficient mice-derived xenograft models have been widely used in cancer drug research; however, these models have some limitations, including i) they are time-consuming and expensive, ii) their use needs to be approved by animal experimental ethics committees, and iii) the inability to visualize where tumor cells or tissues were engrafted. The present study performed a chorioallantoic membrane (CAM) assay in fertilized chicken eggs, which is time-saving, simple, and easy to standardize and handle because of the high vascularization and the immature immune system of the fertilized eggs. The present study aimed to examine the usability of the CAM assay as a novel therapeutic model for the development of precision medicine for pediatric cancer. A protocol was developed for constructing cell line-derived xenograft (CDX) models using a CAM assay by transplanting RMS cells on the CAM. It was then examined as to whether these CDX models could be used as therapeutic drug evaluation models using vincristine (VCR) and human RMS cell lines. After grafting and culturing the RMS cell suspension on the CAM, three-dimensional proliferation over time was observed visually and by comparing volumes. VCR reduced the size of the RMS tumor on the CAM in a dose-dependent manner. Currently, treatment strategies based on patient-specific oncogenic backgrounds have not been adequately developed in the field of pediatric cancer. The establishment of a CDX model with the CAM assay may lead to the advancement of precision medicine and help formulate novel therapeutic strategies for intractable pediatric cancer.

Correspondence to: Dr Ken Kikuchi, Department of Pediatrics, Graduate School of Medical Science, Kyoto Prefectural University of Medicine, 465 Kajii-Cho, Kawaramachi-Hirokoji, Kamigyo-ku, Kyoto 602-8566, Japan
E-mail: ken-k@koto.kpu-m.ac.jp

Abbreviations: ARMS, alveolar RMS; CAM, chorioallantoic membrane; CDX, cell line-derived xenograft; D-luciferin, D-luciferin potassium salt; ERMS, embryonal RMS; H&E, hematoxylin and eosin; IHC, immunohistochemistry; PBS, phosphate-buffered saline; PDX, patient-derived xenograft; RMS, rhabdomyosarcoma

Key words: RMS, CAM assay, CDX model, 3R principle, alternative model, precision medicine

Introduction

Drug sensitivity and the severity of side effects vary from patient to patient; therefore, it is necessary to develop precision medicine designed to provide the optimal type and amount of treatment for each patient. The development of precision medicine based on patient genetic information has markedly improved therapeutic methods for some types of adult cancer, such as chronic myelocytic leukemia and breast cancer; however, precision medicine for pediatric cancer has not been fully developed because of its rarity and diversity (1).

Immunodeficient mouse models, cell-derived xenograft (CDX) models and patient-derived xenograft (PDX) models have been commonly used for cancer drug research; however, these murine models have some weaknesses: i) Establishment and maintenance of a PDX model is time-consuming and a high cost is incurred to manage its quality, ii) experimental procedures should be undertaken to reduce the number of animals used per study or to refine procedures to improve animal welfare, and iii) it is impossible to visualize the site of xenografts (2-5).

The chorioallantoic membrane (CAM) is an extraembryonic membrane consisting of chorion and allantois in fertilized chicken eggs. The CAM assay has been widely used to study angiogenesis, infiltration and metastasis using human-, rodent- and bird-derived xenografts (6-9). The CAM assay has the following advantages compared with conventional PDX models: i) High vascularization and an immature immune system enable the establishment of time-saving and easy-to-handle PDX models (3,4,10,11), ii) chick embryos are

not specified as laboratory animals in a number of countries, which support compliance with the 3R principle of animal research (replacement, reduction and refinement) (11-13), iii) the CAM can be visually observed by peeling the shell membrane, which allows the visualization of blood vessels and xenografts. The CAM assay is thus considered a suitable model to evaluate the biological and pharmacological characteristics of tumor tissues.

Rhabdomyosarcoma (RMS) is the most common type of highly malignant pediatric soft tissue sarcoma in the United States (≥50% of pediatric soft tissue sarcomas) (14,15). The two major subtypes of pediatric RMS, embryonal RMS (ERMS) and alveolar RMS (ARMS), have some differences in histopathological features, age of onset, site of primary lesions and expression of fused genes, which are utilized for the diagnosis and classification of risk groups (15-19). The prognosis is less favorable in fusion-positive ARMS (80% of patients with ARMS) than ERMS (14,17,20). However, fusion-negative ARMS is genetically and critically similar to ERMS (21,22).

Progress in multidisciplinary treatment has improved the 5-year survival rate of low/intermediate-risk patients to 70-90%, but that of high-risk patients remains <30% in the United States (23-25). While the survival rate has improved, it remains a serious problem that nonspecific high-dose chemotherapy and radiotherapy can cause various complications at later stages of life, including facial deformity, growth hormone deficiency, fertility disorders and secondary cancer (26-29).

The present study aimed to explore whether the CAM assay is a novel treatment model that could contribute to precision medicine for pediatric cancer. As a first step, this study aimed to establish a protocol for the CAM assay with transplantation of RMS cells on the CAM and examined how to evaluate the effect of anticancer drugs.

Materials and methods

Cell culture and reagents. The present study was approved by the Institutional Gene Recombination Experimentation Committee of the Kyoto Prefectural University of Medicine (approval no. #2019-35; Kyoto, Japan). The human ERMS cell line RD was purchased from the Japanese Collection of Research Bioresources Cell Bank, and the human ARMS cell line SJ-Rh30 was kindly provided by Dr Peter J. Houghton (Greehey Children's Cancer Research Institute, University of Texas Health Science Center, San Antonio, TX, USA) (30). Firefly luciferase-expressing RD and SJ-Rh30 were established by transducing RediFect Red-Luc-Puromycin lentiviral particles (PerkinElmer, Inc.) into the cells. Briefly, RD and SJ-Rh30 cells were plated at $5.0x10^5$ cells/100-mm dish. After 24 h, hexadimethrine bromide was added (8 mg/ml; cat. no, H9268; MilliporeSigma), followed by each particle solution (MOI, 0.5). After another 24 h, media were removed and fresh media were added. The following day, puromycin was added (5 mg/ml; cat. no. P8833; MilliporeSigma). Puromycin-resistant clones were selected with cloning rings at day 14, with continuous puromycin selection at all times. Cell lines were cultured in Dulbecco's modified Eagle's medium (4.5 g/l glucose) (Nacalai Tesque, Inc.) containing 10% fetal bovine serum (Gibco; Thermo Fisher Scientific, Inc.) and 1 μg/ml puromycin (Thermo Fisher Scientific, Inc.) at 37˚C under a 5% CO_2 atmosphere in an incubator. Vincristine (VCR) (cat. no. S1241; Selleck Chemicals) was dissolved in dimethyl sulfoxide (cat. no. D2950; MilliporeSigma) and stored as a 1 mM stock solution at -20˚C. D-Luciferin potassium salt (D-luciferin; cat. no. 12507; AAT Bioquest, Inc.) was dissolved in phosphate-buffered saline (PBS; Nacalai Tesque, Inc.) and stored as a 15 mg/ml stock solution at -20˚C. The cells were screened periodically for mycoplasma contamination using a Mycoplasma Detection kit (MycoStrip™; Invivogen).

Chick CAM assay. A total of 350 fertilized eggs from a local commercial hatchery were incubated in an upright position at 37˚C and 60% humidity. The day the eggs were kept in the incubator was designated as day 0 (Fig. 1A). On day 9, a small hole was made in the air chamber side of the eggshell with an egg piercer and surgical scissors after tracing the edges of the air chamber with a pencil under illumination in a darkroom. The eggshell membrane was removed with tweezers and a sterile silicon ring (inner diameter, 5 mm) was placed at the center of the CAM (Fig. 1B-F). Tumor cells were detached from culture dishes using trypsin/ethylenediaminetetraacetic acid and were counted. Cell line suspensions were resuspended in Matrigel and PBS (3:1 ratio) at $2.0x10^6$ cells/25 μl Matrigel solution and the mixture was directly pipetted into the center of the ring (Fig. 1G and I). The hole was resealed with parafilm and the eggs were placed in the incubator (Fig. 1H). Successful development of cell xenografts was confirmed by visual observation and chemiluminescent imaging with the G:BOX Chemi XRQ gel doc system (Syngene International, Ltd.). On days 12, 14, 16 and 18,50 μl D-luciferin was added to cell xenografts before chemiluminescent imaging (D-luciferin was thawed and diluted to 1:100 with Dulbecco's modified Eagle's medium before use). On days 14, 16 and 18, the xenograft tumors were resected, and the length of three sides was measured with a vernier caliper and the product of the lengths of three sides was taken as the volume (length x width x height). For the control immunostaining samples, the leg muscular tissues from one chick embryo were also resected on day 16. Chick embryos were euthanized by an overdose of pentobarbital (100 mg/kg) before resection of the xenograft tumors. The excised tumors were fixed with 100% formalin overnight at room temperature and paraffin-embedded for hematoxylin and eosin (H&E) staining. Paraffin-embedded sections (4 μm) were deparaffinized in xylene and rehydrated in ethanol after incubation on a paraffin spreading unit at 65˚C for 15 min. The sections were stained with hematoxylin (6.5 min) and eosin (1 min) at room temperature, and the slides were observed under a light microscope.

Immunohistochemistry (IHC). Formalin-fixed paraffin-embedded chick embryo tissues and CAM assay xenografts were deparaffinized in xylene and rehydrated in ethanol. IHC was performed using an anti-human vimentin antibody (1:200; cat. no. ab16700; Abcam). Blocking, HRP micro-polymer secondary antibody incubation and DAB detection were performed using a rabbit-specific HRP/DAB Detection IHC Kit (cat. no. ab236469; Abcam). The sections were blocked with Protein Block for 10 min at room temperature and incubated with primary antibody overnight at 4˚C. After blocking with 3% hydrogen peroxide for 10 min at room temperature,

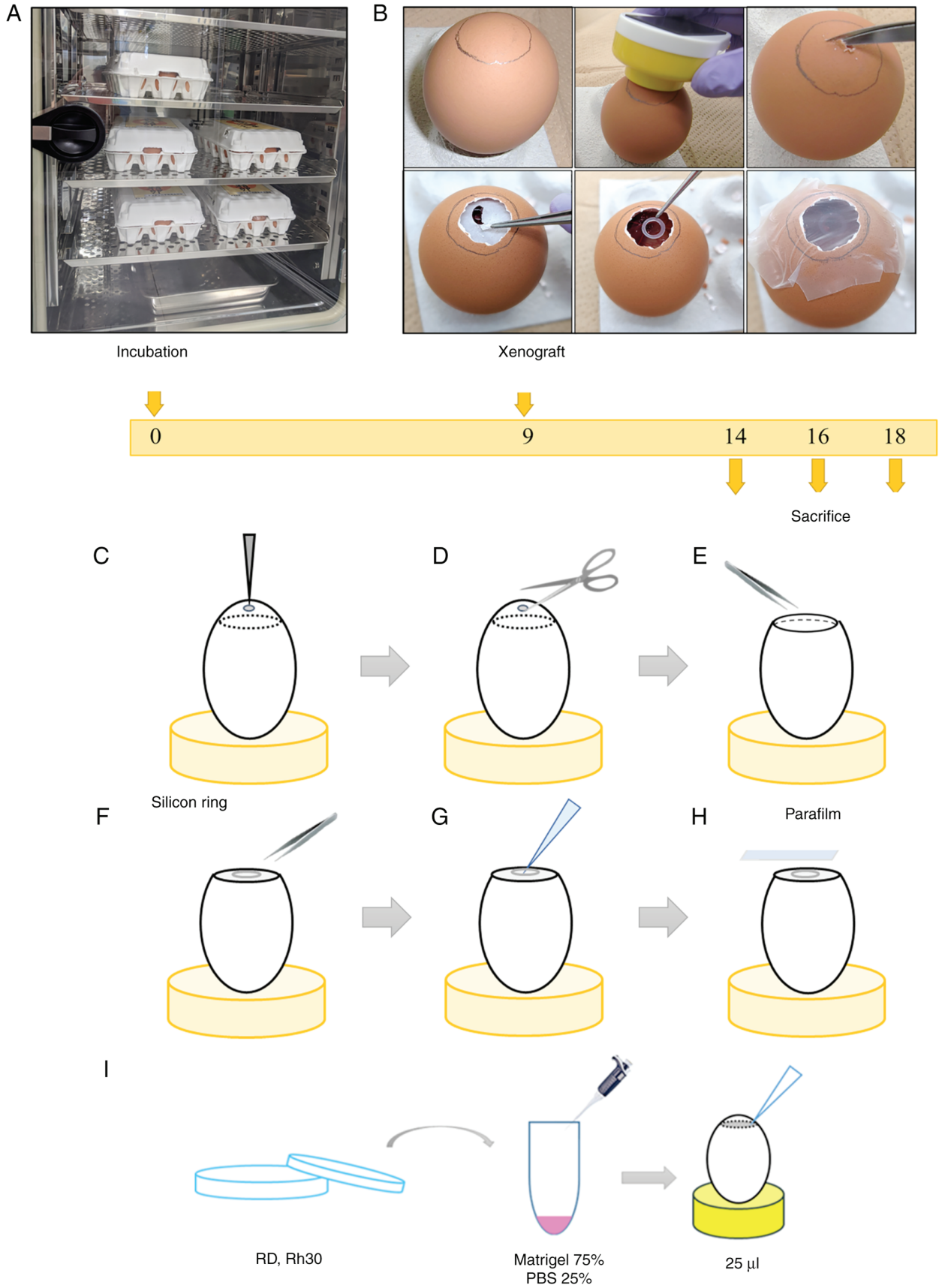

Figure 1. Diagram of cell-derived xenograft model generation using the CAM assay. (A) Day 0. Commercial fertilized eggs were placed upright in an incubator at 37˚C and 60% humidity. (B) Day 9. Photographs of steps (C-H). Prior to step C, the edges of the air chamber were traced with a pencil while illuminating the eggs in the darkroom. (C) A hole was made on top of the egg with an egg piercer. (D) Scissors were used to cut the shell along the edge of the air chamber. (E) Eggshell membrane was removed with tweezers. (F) A silicon ring was placed on the CAM. (G) A cell suspension (25 μl) was grafted onto the CAM. (H) After cell inoculation, the window in the egg was tightly sealed using parafilm and the eggs were returned to the incubator. (I) Cell suspension was prepared by detaching tumor cells from culture dishes using trypsin/ethylenediaminetetraacetic acid and counting them. The cells were resuspended in Matrigel and PBS (3:1 ratio) at 2.0x10^6 cells/25 μl Matrigel solution. CAM, chorioallantoic membrane; PBS, phosphate-buffered saline.

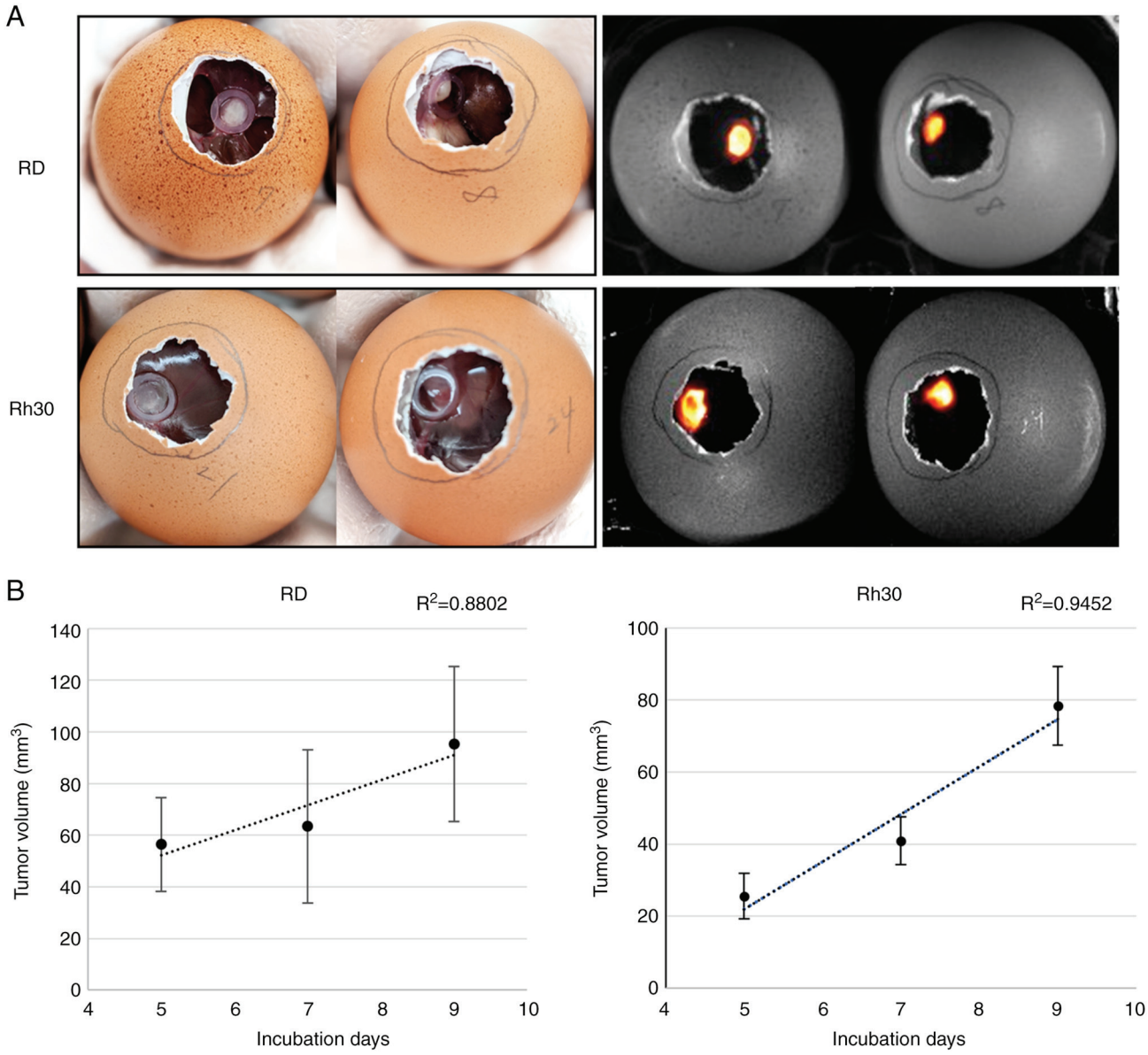

Figure 2. Continued.

incubation with secondary antibody was performed for 20 min at room temperature. DAB detection was performed for 3 min at room temperature and nuclei were counterstained with 3% methyl green for 20 min at room temperature (cat. no. 12001; Muto Pure Chemicals Co. Ltd.). The slides were observed under a light microscope.

WST-8 cell viability assay. WST-8 colorimetric assays were performed using a Cell Counting Kit-8 (Dojindo Laboratories, Inc.) according to the manufacturer's instructions. RD cells were plated in a 96-well plate at a density of $5.0x10^3$/well in 80 μl culture media. After 24 h, dimethyl sulfoxide or VCR (1 pM-1 μM) was added to each well. Cell viability was determined every 24 h after treatment with VCR by measuring the absorbance at 450 nm using a microplate reader (Multiscan JX; Sumitomo Pharma Co., Ltd.). The dose-response curve was generated using ImageJ (National Institutes of Health; version 1.52a). The mean half-maximal inhibitory concentration (IC_{50}) was calculated based on the dose-response curve on day 3.

Statistical analysis. All data are presented by the mean ± standard error. The statistical significance of differences between samples was determined using one-way ANOVA and Dunnett's post hoc test. $P<0.05$ was considered to indicate a statistically significant difference. R^2 values were calculated using the least-squares method. All statistical analyses were performed with EZR (Saitama Medical Center, Jichi Medical University, Saitama, Japan), which is a graphical user interface for R (The R Foundation for Statistical Computing; version 1.40) (31).

Results

Establishment of a RSM model using the CAM assay. As shown in Fig. 1, day 0 was defined as the day when the commercial fertilized eggs were kept in the incubator and a hole was made in the eggshell on day 9. A total of 7 days after transplantation with firefly-expressing RD and Rh30 cells onto the CAM, both tumors formed a mass that could be visualized

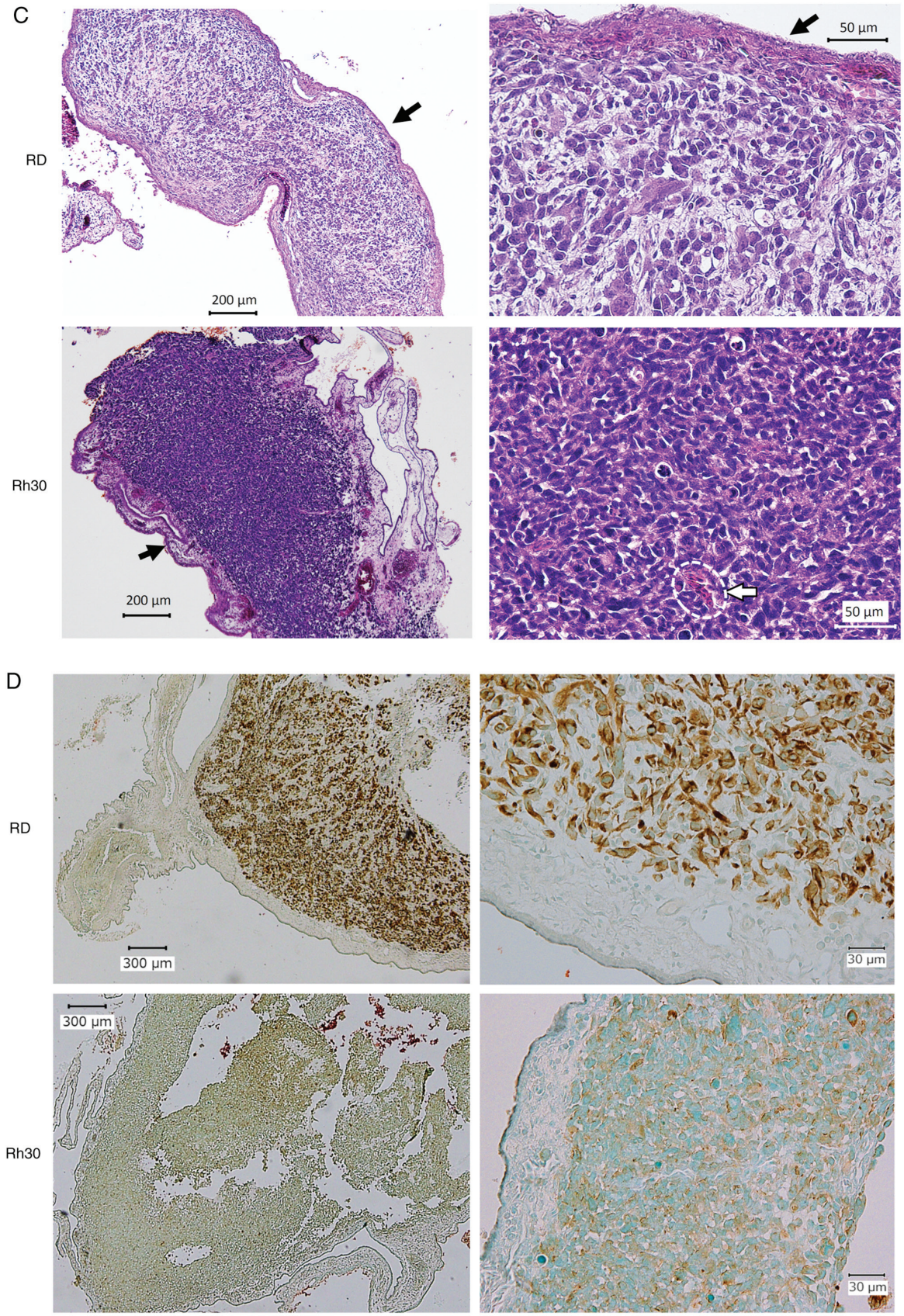

Figure 2. Establishment of a cell-derived xenograft model on the CAM using the RMS cell lines, RD and Rh30. (A) Tumor formed on the CAM on day 16 (7 days after transplantation of RD or Rh30 cells). Images on the left were captured on a clean bench, whereas images on the right were observed using the G:BOX Chemi XRQ gel doc system following the addition of luciferin. (B) Temporal changes in tumor volume. Tumors were resected on days 14, 16 and 18, and the volume was calculated using Vernier caliper measurements. (C) Hematoxylin and eosin staining of the resected tumors on day 16 (left, x40 magnification; right, x200 magnification). Accumulation of cells and formation of RMS tissue along the CAM (black arrow), and infiltration of some chick red blood cells into the tissue (inside white dotted line) were observed. (D) Immunohistochemical staining of anti-human vimentin in the tumor tissue (left, x40 magnification; right, x200 magnification). Counterstaining of sections was performed with methyl green. These results indicated that the resected tumor consisted of human RMS cells transplanted on day 9. CAM, chorioallantoic membrane; RMS, rhabdomyosarcoma.

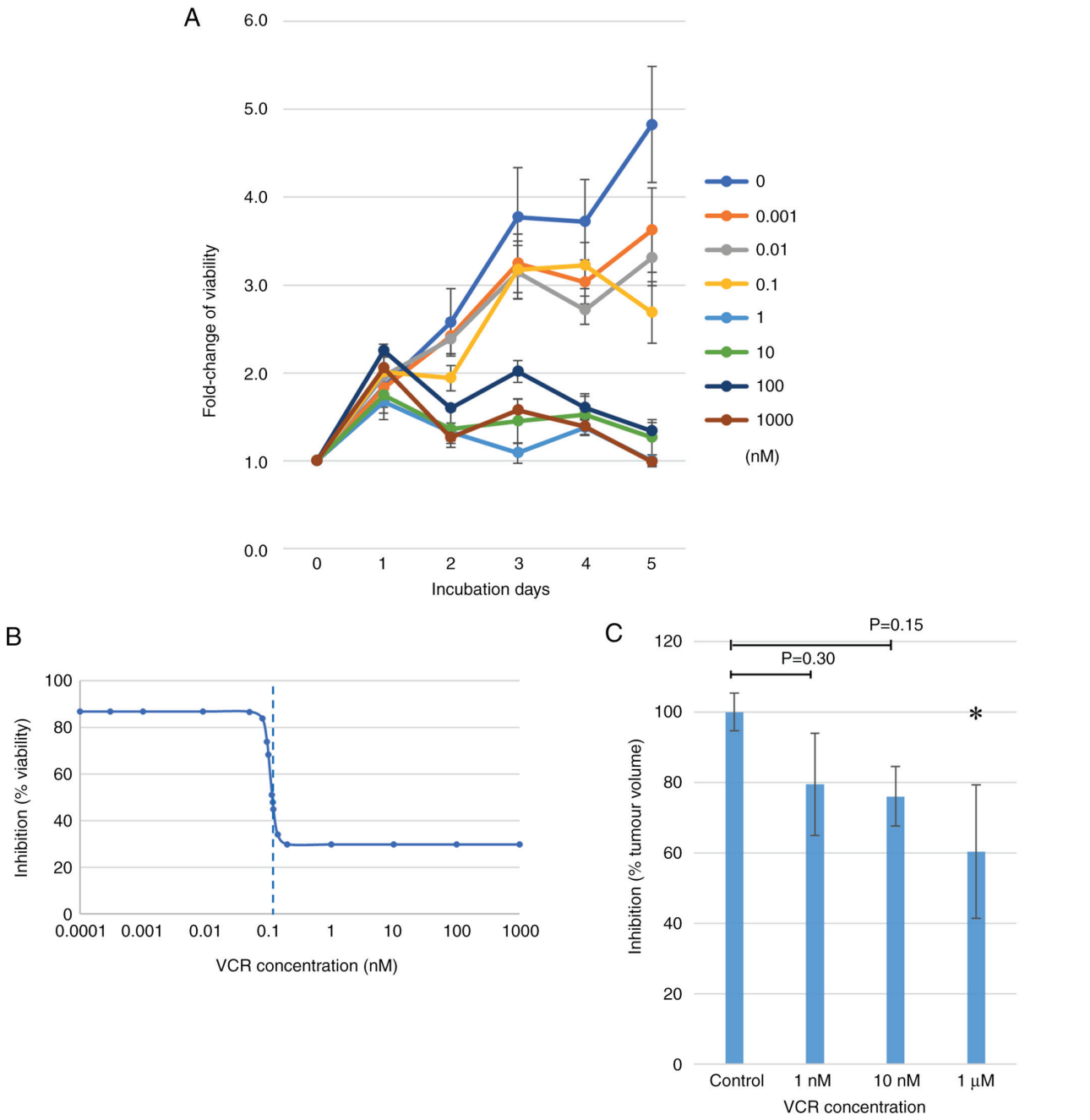

Figure 3. Continued.

by adding D-luciferin (Fig. 2A). The xenograft tumors were resected and their volume was calculated using measurements obtained with a Vernier caliper on days 14, 16 and 18 (i.e., 5, 7 and 9 days after xenograft generation on the CAM). The RD and Rh30 cell-derived tumors increased temporally and three-dimensionally over time (Fig. 2B). In addition, pathological analysis of the tumor tissue on day 16 was performed, which confirmed that tumor cells were densely aggregated along the CAM (Fig. 2C, black arrows), with the invasion of chick blood cells with prominent nuclei (32) (Fig. 2C, white dotted line) suggesting the formation of feeding vessels from the CAM. Tumor cells were positive for human-specific vimentin and CAM was negative as confirmed by IHC (Fig. 2D), which indicated the RMS characteristics of these tumor masses. Notably, human vimentin antibodies did not cross-react with chicken tissues (Fig. S1; Data S1), indicating that IHC for human vimentin could discriminate between the human RMS-derived tissue and chicken muscular tissues.

Utilization of the CAM assay for anticancer drug screening. VCR is one of the key chemotherapeutic agents for RMS and is widely used to treat RMS. For the anticancer drug screening using the RD-derived tumor established on the CAM, the present study first evaluated the sensitivity of VCR against RD cells using the WST-8 cell viability assay (Fig. 3A). The IC_{50} of VCR was 0.114 nM and a clear decrease in the viability of RD cells was detected when they were treated with >1 nM VCR (Fig. 3B). Based on these results, the concentrations of VCR for the treatment of RD-derived tumors on the CAM were selected. Briefly, the RD cell suspension was grafted

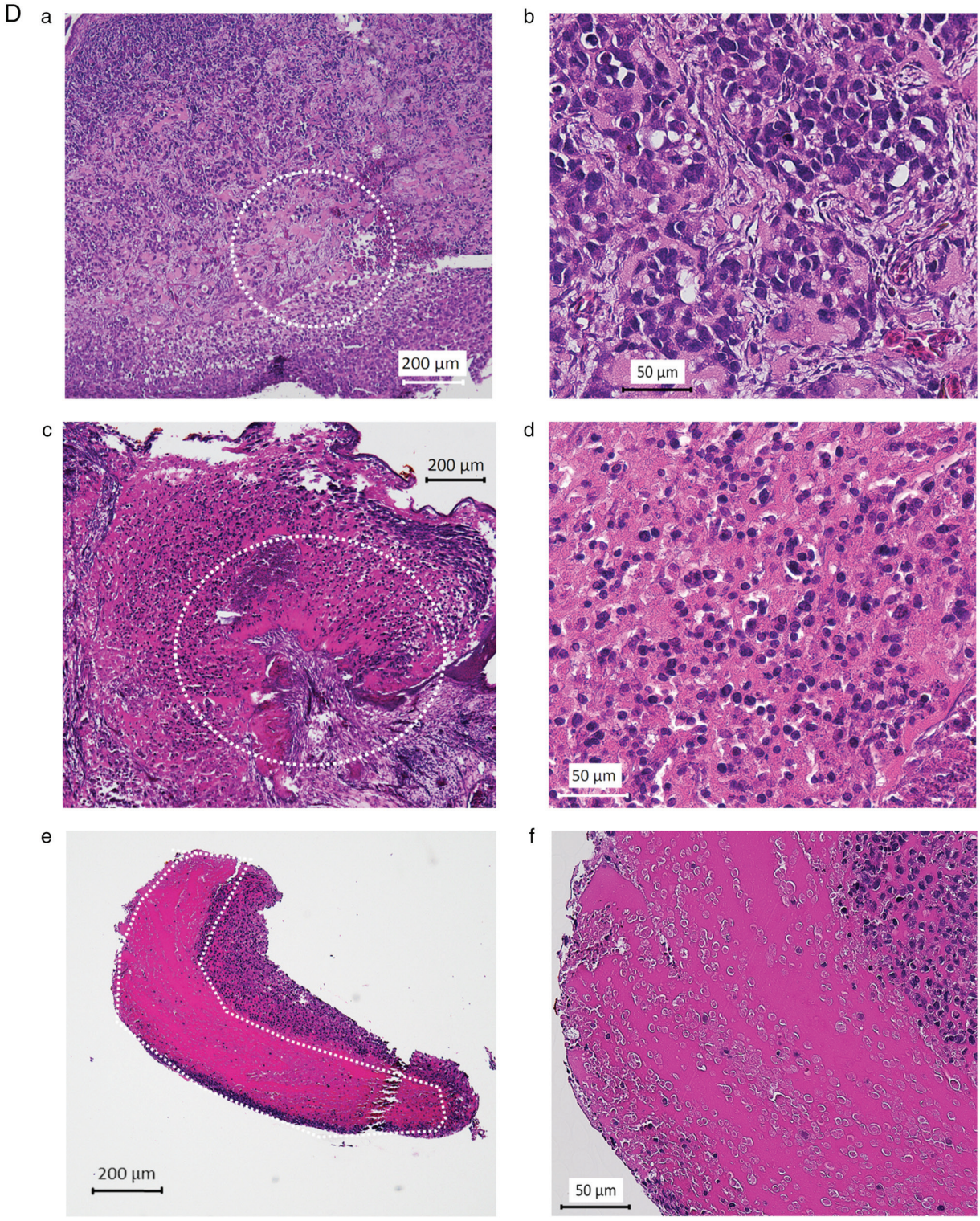

Figure 3. Administration of VCR resulted in a reduction in tumor volume on the CAM. (A and B) Results of the WST-8 assay. (A) Cell viability curve (VCR concentration, 0 pM-1 μM). (B) Viability inhibition curve on day 3. Half-maximal inhibitory concentration, 0.114 nM (dotted line). (C) Changes in tumor volume due to different concentrations of VCR administration. RD cells were grafted on the CAM on day 9 and 100 μl VCR was administered to each tumor on day 12. On day 16, tumors were resected and volumes were calculated. Data are presented as the mean ± standard error of three independent experiments. Data were analyzed using one-way ANOVA (P=0.0306), followed by Dunnett's post hoc test. *P<0.05 vs. control. (D) Hematoxylin and eosin staining of resected tumors. Necrotic area expansion was VCR concentration-dependent; necrotic areas are outlined with a white dotted line. Xenografts were treated with (a and b) 1 nM, (c and d) 10 nM and (e and f) 1 μM VCR. (a, c and e) x40 magnification; (b, d and f) x200 magnification. CAM, chorioallantoic membrane; VCR, vincristine.

on the CAM on day 9. The implanted eggs were then divided into three groups, and 1 nM, 10 nM or 1 μM VCR was placed directly on the RD-derived tumors on day 12 (3 days after xenograft generation). Tumors were resected on day 16 for further evaluation. It was observed that the volume of resected tumors decreased in a concentration-dependent manner

(Fig. 3C). Furthermore, it was observed that the range of necrotic tissue spread in a concentration-dependent manner (Fig. 3D); suggesting that the RD-derived tissue on the CAM was sensitive to VCR and the findings were similar to those obtained from the *in vitro* drug-sensitivity assay.

Discussion

The present study established a CDX model using a CAM assay with the human ERMS cell line, RD, and the ARMS cell line, Rh30. The formation of a three-dimensional tumor mass on the CAM was confirmed by visual observation and the temporal multiplication of grafted cells by calculating the volume using a Vernier caliper. Moreover, pathological assessments confirmed that transplanted cells gathered and formed tumor tissue along the CAM. Some chick red blood cells infiltrated the tissue, indicating that the transplanted cells were nourished by the chick host and that the CAM assay was helpful in the establishment of CDX models. Moreover, tumors on the CAM were sensitive to VCR in a concentration-dependent manner, confirming the utility of the CAM assay as a therapeutic model both three-dimensionally and histologically. Therefore, the CAM assay could be useful to determine the sensitivity of anticancer drugs.

The CAM assay has been widely used in the research field of oncological morphology; however, the protocol of tumor engraftment is not standardized. Some researchers have placed the fertilized eggs horizontally (10,13), whereas others have created *ex ovo* xenograft models by transferring chick embryos onto sterilized trays (12,33). After trying the former method several times, it was revealed that the CAM was often damaged during the process of punching holes in the eggshells. In addition, there was often a considerable difference between the area of the hole on the eggshell and the range of motion of the tumor on the CAM, which made it challenging to observe the tumors on the CAM. The *ex ovo* method was previously reported to lower the chick embryo survival ratio compared with the *in ovo* method (2). The present study adopted a method of using fertilized eggs placed vertically due to its simplicity and stability. The time taken for cell line transplantation and tumor resection to minimize damage to the CAM and improve the survival rate of chick embryos was determined by referring to previous reports (10,13). To help the local formation of spherical tumors, silicone rings were placed on the CAM and the cell suspension was added to their center.

Although we initially tried to assess how grafted RMS cells multiplied on the CAM through fluorescence analysis using luciferase-transgenic cell lines, we shifted to calculating the volume of resected tumors with measurements using Vernier calipers because the results of this assessment were revealed to be consistent with those of H&E staining. Fluorescence analysis was limited to two dimensions in the range visible through the hole in the eggshell, and was easily influenced by tumor crookedness and movement under the eggshell related to embryo motion.

The CAM assay has a number of advantages over mouse models. First, it is time- and cost-effective, whereas mouse models require long observation periods (weeks to months) (16,17,34), the CAM assay is completed within 10 days after cell xenograft. The CAM assay can also assess the effectiveness of chemotherapy agents more rapidly. Second, chick embryos are not regarded as animals in numerous countries, and CAM assay experiments do not require the approval of animal experimental ethics committees. Furthermore, the CAM is not innervated, thus preventing the infliction of pain and suffering on the chick embryos (10). Third, the CAM can be seen directly, so that it is possible to not only visualize the sites of tumor cells or tissues xenografts and drug administration but also to easily observe the development of tumors on the CAM and therapeutic efficacy.

In the field of pediatric cancer, the use of precision medicine has made less progress than in adult cancer, and a remedy based on the oncogenic background of patients has not yet been established. Previous studies have applied the CAM assay as an alternative model for RMS studies (35-38); however, these studies have not mentioned the application of this model to precision medicine. In addition, other studies have investigated how to take advantage of the CAM assay for precision medicine (3,4), yet these studies have not assessed RMS. It may be hypothesized that the RMS CDX model described in the present study using the CAM assay has the potential to substantiate and develop novel patient-specific therapeutic medicines, and may become the foundation of precision medicine for RMS and intractable pediatric cancer.

The present study has some limitations. First, only one cell line was examined for each ERMS and ARMS; in the future, we aim to examine other RMS cell lines. Second, the less damaging method of administering VCR via intravenous injection could not adequately be examined.

In conclusion, the present study established a CAM assay protocol using human RMS cell lines and confirmed the formation of a three-dimensional tumor mass on the CAM. Moreover, the anticancer efficacy of VCR was demonstrated on established human RMS CDX models. The CAM assay may therefore be useful as both a CDX model and a therapeutic model. In the future, we aim to establish CDX models using other RMS cell lines and PDX models using tumor tissue resected from mouse CDX models or patients, and to examine the utility of the models.

Acknowledgements

The authors would like to thank Dr Peter J. Houghton, (Greehey Children's Cancer Research Institute, University of Texas Health Science Center, San Antonio, TX, USA) for providing the Rh30 cell line. The authors are also grateful to Dr Satoshi Miyagaki, Dr Akihiro Nishida and Ms. Mami Kotoura (Department of Pediatrics, Graduate School of Medical Science, Kyoto Prefectural University of Medicine, Kyoto, Japan) for teaching us the experimental techniques.

Funding

This work was supported by a grant from JSPS KAKENHI (grant no. JP 20K08187).

Availability of data and materials

The datasets used and/or analyzed during the current study are available from the corresponding author on reasonable request.

Authors' contributions

CS performed the experiments. KK and TI designed this study and confirmed the authenticity of all the raw data. CS, KK, HY, MM, SY, KT and HH interpreted and processed the experimental data, and performed the analysis. TN contributed to the original technical methods using CAM. CS, KK, HY, MM, SY, KT, TN, HH and TI discussed the results and contributed to the final manuscript. All authors read and approved the final manuscript.

Ethics approval and consent to participate

This study was approved by the Faculty of Science Ethics Committee of the Kyoto Prefectural University of Medicine (approval no. #2019-35).

Patient consent for publication

Not applicable.

Competing interests

The authors declare that they have no competing interests.

References

1. Do K, O'Sullivan Coyne G and Chen AP: An overview of the NCI precision medicine trials-NCI MATCH and MPACT. Chin Clin Oncol 4: 31, 2015.
2. Lokman NA, Elder ASF, Ricciardelli C and Oehler MK: Chick chorioallantoic membrane (CAM) assay as an in vivo model to study the effect of newly identified molecules on ovarian cancer invasion and metastasis. Int J Mol Sci 13: 9959-9970, 2012.
3. DeBord LC, Pathak RR, Villaneuva M, Liu HC, Harrington DA, Yu W, Lewis MT and Sikora AG: The chick chorioallantoic membrane (CAM) as a versatile patient-derived xenograft (PDX) platform for precision medicine and preclinical research. Am J Cancer Res 8: 1642-1660, 2018.
4. Chu PY, Koh AP, Antony J and Huang RY: Applications of the chick chorioallantoic membrane as an alternative model for cancer studies. Cells Tissues Organs 211: 222-237, 2022.
5. Valdes TI, Kreutzer D and Moussy F: The chick chorioallantoic membrane as a novel in vivo model for the testing of biomaterials. J Biomed Mater Res 62: 273-282, 2002.
6. Ribatti D: Chicken chorioallantoic membrane angiogenesis model. Methods Mol Biol 843: 47-57, 2012.
7. Fiorentzis M, Viestenz A, Siebolts U, Seitz B, Coupland SE and Heinzelmann J: The potential use of electrochemotherapy in the treatment of uveal melanoma: In vitro results in 3D tumor cultures and in vivo results in a chick embryo model. Cancers (Basel) 11: 1344, 2019.
8. Moreno-Jiménez I, Lanham SA, Kanczler JM, Hulsart-Billstrom G, Evans ND and Oreffo ROC: Remodelling of human bone on the chorioallantoic membrane of the chicken egg: De novo bone formation and resorption. J Tissue Eng Regen Med 12: 1877-1890, 2018.
9. Rasmussen SV, Berlow NE, Price LH, Mansoor A, Cairo S, Rugonyi S and Keller C: Preclinical therapeutics ex ovo quail eggs as a biomimetic automation-ready xenograft platform. Sci Rep 11: 23302, 2021.
10. Kunz P, Schenker A, Sähr H, Lehner B and Fellenberg J: Optimization of the chicken chorioallantoic membrane assay as reliable in vivo model for the analysis of osteosarcoma. PLoS One 14: e0215312, 2019.
11. Ribatti D: The chick embryo chorioallantoic membrane (CAM) assay. Reprod Toxicol 70: 97-101, 2017.
12. Nowak-Sliwinska P, Segura T and Iruela-Arispe ML: The chicken chorioallantoic membrane model in biology, medicine and bioengineering. Angiogenesis 17: 779-804, 2014.
13. Vu BT, Shahin SA, Croissant J, Fatieiev Y, Matsumoto K, Le-Hoang Doan T, Yik T, Simargi S, Conteras A, Ratliff L, *et al*: Chick chorioallantoic membrane assay as an in vivo model to study the effect of nanoparticle-based anticancer drugs in ovarian cancer. Sci Rep 8: 8524, 2018.
14. Dasgupta R, Fuchs J and Rodeberg D: Rhabdomyosarcoma. Semin Pediatr Surg 25: 276-283, 2016.
15. Ognjanovic S, Linabery AM, Charbonneau B and Ross JA: Trends in childhood rhabdomyosarcoma incidence and survival in the United States, 1975-2005. Cancer 115: 4218-4226, 2009.
16. Nakagawa N, Kikuchi K, Yagyu S, Miyachi M, Iehara T, Tajiri T, Sakai T and Hosoi H: Mutations in the RAS pathway as potential precision medicine targets in treatment of rhabdomyosarcoma. Biochem Biophys Res Commun 512: 524-530, 2019.
17. Ouchi K, Miyachi M, Yagyu S, Kikuchi K, Kuwahara Y, Tsuchiya K, Iehara T and Hosoi H: Oncogenic role of HMGA2 in fusion-negative rhabdomyosarcoma cells. Cancer Cell Int 20: 192, 2020.
18. Gurria JP and Dasgupta R: Rhabdomyosarcoma and extraosseous ewing sarcoma. Children (Basel) 5: 165, 2018.
19. Malempati S and Hawkins DS: Rhabdomyosarcoma: Review of the children's oncology group (COG) soft-tissue sarcoma committee experience and rationale for current COG studies. Pediatr Blood Cancer 59: 5-10, 2012.
20. Otabe O, Kikuchi K, Tsuchiya K, Katsumi Y, Yagyu S, Miyachi M, Iehara T and Hosoi H: MET/ERK2 pathway regulates the motility of human alveolar rhabdomyosarcoma cells. Oncol Rep 37: 98-104, 2017.
21. Davicioni E, Anderson MJ, Finckenstein FG, Lynch JC, Qualman SJ, Shimada H, Schofield DE, Buckley JD, Meyer WH, Sorensen PH and Triche TJ: Molecular classification of rhabdomyosarcoma-genotypic and phenotypic determinants of diagnosis: A report from the children's oncology group. Am J Pathol 174: 550-564, 2009.
22. Williamson D, Missiaglia E, de Reyniès A, Pierron G, Thuille B, Palenzuela G, Thway K, Orbach D, Laé M, Fréneaux P, *et al*: Fusion gene-negative alveolar rhabdomyosarcoma is clinically and molecularly indistinguishable from embryonal rhabdomyosarcoma. J Clin Oncol 28: 2151-2158, 2010.
23. Meza JL, Anderson J, Pappo AS and Meyer WH; Children's Oncology Group: Analysis of prognostic factors in patients with nonmetastatic rhabdomyosarcoma treated on intergroup rhabdomyosarcoma studies III and IV: The children's oncology group. J Clin Oncol 24: 3844-3851, 2006.
24. Arndt CAS, Stoner JA, Hawkins DS, Rodeberg DA, Hayes-Jordan AA, Paidas CN, Parham DM, Teot LA, Wharam MD, Breneman JC, *et al*: Vincristine, actinomycin, and cyclophosphamide compared with vincristine, actinomycin, and cyclophosphamide alternating with vincristine, topotecan, and cyclophosphamide for intermediate-risk rhabdomyosarcoma: Children's oncology group study D9803. J Clin Oncol 27: 5182-5188, 2009.
25. Oberlin O, Rey A, Lyden E, Bisogno G, Stevens MC, Meyer WH, Carli M and Anderson JR: Prognostic factors in metastatic rhabdomyosarcomas: Results of a pooled analysis from United States and European cooperative groups. J Clin Oncol 26: 2384-2389, 2008.
26. Arndt CAS, Rose PS, Folpe AL and Laack NN: Common musculoskeletal tumors of childhood and adolescence. Mayo Clin Proc 87: 475-487, 2012.
27. Lockney NA, Friedman DN, Wexler LH, Sklar CA, Casey DL and Wolden SL: Late toxicities of intensity-modulated radiation therapy for head and neck rhabdomyosarcoma. Pediatr Blood Cancer 63: 1608-1614, 2016.
28. Clement SC, Schoot RA, Slater O, Chisholm JC, Abela C, Balm AJM, van den Brekel MW, Breunis WB, Chang YC, Davila Fajardo R, *et al*: Endocrine disorders among long-term survivors of childhood head and neck rhabdomyosarcoma. Eur J Cancer 54: 1-10, 2016.
29. Walterhouse D and Watson A: Optimal management strategies for rhabdomyosarcoma in children. Paediatr Drugs 9: 391-400, 2007.
30. Douglass EC, Valentine M, Etcubanas E, Parham D, Webber BL, Houghton PJ, Houghton JA and Green AA: A specific chromosomal abnormality in rhabdomyosarcoma. Cytogenet Cell Genet 45: 148-155, 1987.
31. Kanda Y: Investigation of the freely available easy-to-use software 'EZR' for medical statistics. Bone Marrow Transplant 48: 452-458, 2013.
32. Schwartz SO and Stansbury F: Significance of nucleated red blood cells in peripheral blood; analysis of 1,496 cases. J Am Med Assoc 154: 1339-1340, 1954.

33. Ghaffari-Tabrizi-Wizsy N, Passegger CA, Nebel L, Krismer F, Herzer-Schneidhofer G, Schwach G and Pfragner R: The avian chorioallantoic membrane as an alternative tool to study medullary thyroid cancer. Endocr Connect 8: 462-467, 2019.
34. Linardic CM, Downie DL, Qualman S, Bentley RC and Counter CM: Genetic modeling of human rhabdomyosarcoma. Cancer Res 65: 4490-4495, 2005.
35. Dolgikh N, Hugle M, Vogler M and Fulda S: NRAS-mutated rhabdomyosarcoma cells are vulnerable to mitochondrial apoptosis induced by coinhibition of MEK and PI3Kα. Cancer Res 78: 2000-2013, 2018.
36. Heinicke U, Kupka J, Fichter I and Fulda S: Critical role of mitochondria-mediated apoptosis for JNJ-26481585-induced antitumor activity in rhabdomyosarcoma. Oncogene 35: 3729-3741, 2016.
37. Asam C, Buerger K, Felthaus O, Brébant V, Rachel R, Prantl L, Witzgall R, Haerteis S and Aung T: Subcellular localization of the chemotherapeutic agent doxorubicin in renal epithelial cells and in tumor cells using correlative light and electron microscopy. Clin Hemorheol Microcirc 73: 157-167, 2019.
38. Abraham J, Prajapati SI, Nishijo K, Schaffer BS, Taniguchi E, Kilcoyne A, McCleish AT, Nelon LD, Giles FG, Efstratiadis A, *et al*: Evasion mechanisms to Igf1r inhibition in rhabdomyosarcoma. Mol Cancer Ther 10: 697-707, 2011.